Two-dimensional image edge enhancement using a spatial frequency filter of two-color radiation

V.M. Kotov

Abstract. **Two-dimensional optical image edge enhancement is investigated using a spatial acousto-optical (AO) filter operating at two wavelengths of optical radiation, which significantly increases the reliability of measurements and also reduces the effect of noise. The filter operates basing on diffraction of light in two diffraction orders. It is shown that, in the general case, it is impossible to obtain a two-dimensional image contour simultaneously at two wavelengths at the same energy and frequency-angular parameters of the AO filter. A regime has been found that makes it possible to switch from one wavelength to another while maintaining the operation of edge enhancement by changing the acoustic power. This regime has been experimentally confirmed by the example of the formation of a two-dimensional image contour using two-colour radiation of an Ar laser emitting at wavelengths of 0.488×10^{-4} and 0.514×10^{-4} cm, and an AO cell made of TeO_2, operating at a sound frequency of 57 MHz.**

Keywords: two-dimensional image edge enhancement, acousto-optic diffraction, two-colour radiation, Bragg regime.

1. Introduction

One of the widely used methods of image processing is its edge enhancement, since this operation makes it possible, on the one hand, to significantly reduce the amount of processed information, and on the other hand, to preserve such important characteristics of an object as its shape, size, nature of movement, etc. For Fourier processing of images, acousto-optic (AO) cells are used as spatial frequency filters due to their high efficiency of influence on the distribution of the optical beam field, rapid adjustment of the diffraction parameters, and the simplicity of the design. However, due to the one-dimensionality of AO diffraction, the first applications of AO filters were associated with the processing of one-dimensional images [1–3]. Later, regimes were found that made it possible to perform two-dimensional processing. These regimes include the regimes of tangential and collinear diffraction geometries [4–8], variants of two- and threefold AO interaction [9–12], as well as regimes of polarisation-independent diffraction [13, 14]. This makes it possible to design filters

V.M. Kotov Kotel'nikov Institute of Radioengineering and Electronics (Fryazino Branch), Russian Academy of Sciences, pl. Vvedenskogo 1, 141190 Fryazino, Moscow region, Russia;
e-mail: vmk277@ire216.msk.su

with different characteristics, designed to process certain types of images.

The above studies were carried out using monochromatic radiation, which is due to the fact that AO Bragg cells have, as a rule, high selectivity with respect to the wavelength of light [15–17]. However, in the early 1990s, works appeared where several regimes of the AO interaction of two-colour radiation with an acoustic wave were proposed (see, for example, [18–21]). Until now, the possibility of using such regimes for processing optical images has not been investigated. Image processing at two wavelengths increases the reliability of measurements, because the characteristics of the medium (its absorption, scattering, etc.) transmitting the image, as well as the spectral characteristics of the image itself, can change with a change in the wavelength of light. In addition, measurements at two wavelengths can significantly lower the effect of noise and interference, reduce the probability of false alarms during automated object recognition, etc.

In this work, an AO cell is considered for the first time as a filter of spatial frequencies of two-colour radiation. The diffraction regime is taken as a basis, when radiation is diffracted into the +1st and −1st diffraction orders [16, 22]. This regime is interesting by the fact that it is realised at substantially lower (approximately two times) acoustic powers compared to the usual diffraction regimes [16].

2. Theory

The vector diffraction diagram underlying the AO filter is shown in Fig. 1. It is assumed that diffraction occurs in a uniaxial gyrotropic crystal, an example of which is a TeO_2 crystal. The surfaces of the wave vectors of the crystal are presented in the three-dimensional Cartesian coordinate system $K_x K_y K_z$, where the K_z axis coincides with the optical axis of the crystal. The acoustic wave propagates along the K_x axis, and the optical radiation propagates near the K_z axis. The inner and outer surfaces of the wave vectors for emissions with wavelengths λ_1 and λ_2 ($\lambda_1 > \lambda_2$) are designated by numbers 1 and 2, respectively. The input optical face of the crystal coincides with the plane $K_z = 0$. The two-colour radiation incident on the optical face splits inside the crystal into monochromatic components with wave vectors K_{01} and K_{02} corresponding to wavelengths λ_1 and λ_2. We assume that the polarisations of the radiation are chosen in such a way that the beams belong to the internal wave surfaces 1. As a result of anisotropic diffraction on an acoustic wave with a wave vector q, beams with K_{01} and K_{02} are diffracted in the direction of the beams belonging to the outer wave surfaces, and the diffraction occurs into the +1st and −1st diffraction orders. The diffracted beams are not shown in Fig. 1 in order not to over-

load it. For simplicity, we consider only the diffraction of radiation with a wavelength λ_1. (Diffraction of radiation with a wavelength λ_2 proceeds in a similar way.) Then the input radiation with a wave vector $\mathbf{K}$ is a monochromatic wave with a wavelength λ_1. It is incident on the crystal face at a certain angle α, with the projections of the vector $\mathbf{K}$ on the K_x and K_y axes being equal to $-K_{x0}$ and $-K_{y0}$. It is clear that these projections completely determine the slope of the vector $\mathbf{K}$ and the orientation of the angle α. In this case, the projections of the vector $\mathbf{K}_{01}$ of the beam refracted in the crystal on the K_x and K_y axes will be equal to K_{x0} and K_{y0} by virtue of Snell's law.
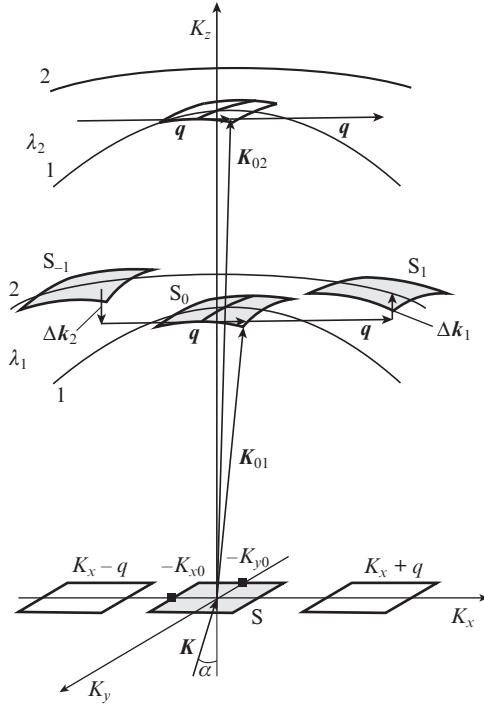

Figure 1. Vector diagram of AO diffraction of two-colour radiation into two diffraction orders.

Let the set of input beams for different angles α contain information about the Fourier transform of some image. This means that the same information is contained in an area S, consisting of a set of points with coordinates $-K_{x0}$ and $-K_{y0}$, as well as an area S_0, 'written' by the end of the vector $\mathbf{K}_{01}$ on the inner surface 1 of the wave vectors. The coordinates of S_0 are K_{x0}, K_{y0}, and K_{z0}, where the projection K_{z0} is related to the projections K_{x0} and K_{y0} by an equation describing the surfaces of the wave vectors of a uniaxial gyrotropic crystal [23]:

$$K_{z0}^4\left(\frac{1}{n_o^4} - G_{33}^2\right) + T_0^2 N\left[\frac{K_{z0}^2}{n_o^2} - \left(\frac{2\pi}{\lambda}\right)^2\right] +$$

$$+\frac{T_0^4}{n_o^2 n_e^2} - \frac{2}{n_o^2}\left(\frac{2\pi}{\lambda}\right)^2 K_{z0}^2 + \left(\frac{2\pi}{\lambda}\right)^4 = 0, \quad (1)$$

where $T_0^2 = K_{x0}^2 + K_{y0}^2$; n_o and n_e are the main refractive indices of the crystal; G_{33} is the component of the gyration pseudotensor $N = n_o^{-2} + n_e^{-2}$; and λ is the wavelength of light. Expressing K_{z0} in terms of T_0 in (1), we obtain a biquadratic equation

$$R_1 K_z^4 - 2P_1 K_z^2 + Q_1 = 0, \quad (2)$$

where

$$R_1 = \frac{1}{n_o^4} - G_{33}^2; \quad P_1 = \frac{1}{2n_o^2}\left[2\left(\frac{2\pi}{\lambda}\right)^2 - T_0^2 N\right];$$

$$\quad (3)$$

$$Q_1 = \frac{T_0^4}{n_o^2 n_e^2} - \left(\frac{2\pi}{\lambda}\right)^2 N T_0^2 + \left(\frac{2\pi}{\lambda}\right)^4.$$

The solution to equation (2) has the form

$$K_{z0(1,2)}^2 = \frac{P_1}{R_1} \pm \sqrt{\left(\frac{P_1}{R_1}\right)^2 - \frac{Q_1}{R_1}}. \quad (4)$$

Here the minus sign describes the inner surface of the wave vectors, and the plus sign describes the outer one. In other words, the incident radiation belongs to the wave surface (4), taken with the minus sign, and the diffracted rays, to the surface (4), taken with the plus sign.

During AO diffraction, radiation with the wave vector $\mathbf{K}_{01}$ is distributed between diffraction orders. Consider diffraction into the +1st order. (Diffraction into the −1st order is described in a similar way.) The radiation diffracted into the +1st order occupies an area S_1, which is formed by a set of points with coordinates $K_{x0} + q$, K_{y0}, and K_{z1}, where the projection K_{z1} is determined from equation (1) with the replacements $K_{x0} \rightarrow K_{x0} + q$ and $K_{y0} \rightarrow K_{y0}$. The diffraction process consists in transferring each point of the area S_0 with coordinates K_{x0}, K_{y0}, and K_{z0} to the corresponding points with coordinates $K_{x0} + q$, K_{y0}, and K_{z1} of the area S_1, while the coordinate K_{z0} is transferred to the coordinate K_{z1} with a shift by $\Delta k_1 = |K_{z1} - K_{z0}|$, called Bragg, or phase-matching detuning. The phase-matching detuning during diffraction into the −1st diffraction order is determined in a similar way. In this case, the detuning is denoted by Δk_2. In Fig. 1, the detunings are shown in the form of vectors $\Delta \mathbf{k}_1$ and $\Delta \mathbf{k}_2$. They play a decisive role in the final distribution of optical fields of both incident and diffracted radiation.

Let E_0, E_1, and E_{-1} be the amplitudes of the waves diffracted in the zero, +1st and −1st diffraction orders. They are related to each other by the system of differential equations [16, 22]:

$$\frac{dE_0}{dz} = -\frac{p}{2}[E_1 \exp(-i\Delta k_1 z) + E_{-1}\exp(-i\Delta k_2 z)],$$

$$\frac{dE_1}{dz} = \frac{p}{2}E_0 \exp(i\Delta k_1 z), \quad (5)$$

$$\frac{dE_{-1}}{dz} = \frac{p}{2}E_0 \exp(i\Delta k_2 z).$$

Here

$$p = \frac{\pi}{\lambda}\sqrt{\frac{M_2 P_{ac}}{LH}}$$

is the parameter associated with the power of the acoustic wave; M_2 is the AO value of the material quality; L and H are the length of the AO interaction and the height of the acoustic column; P_{ac} is the acoustic power; and z is the coordinate along which the AO interaction develops. Solving system (5) in the standard way (see, for example, [23]), we obtain the
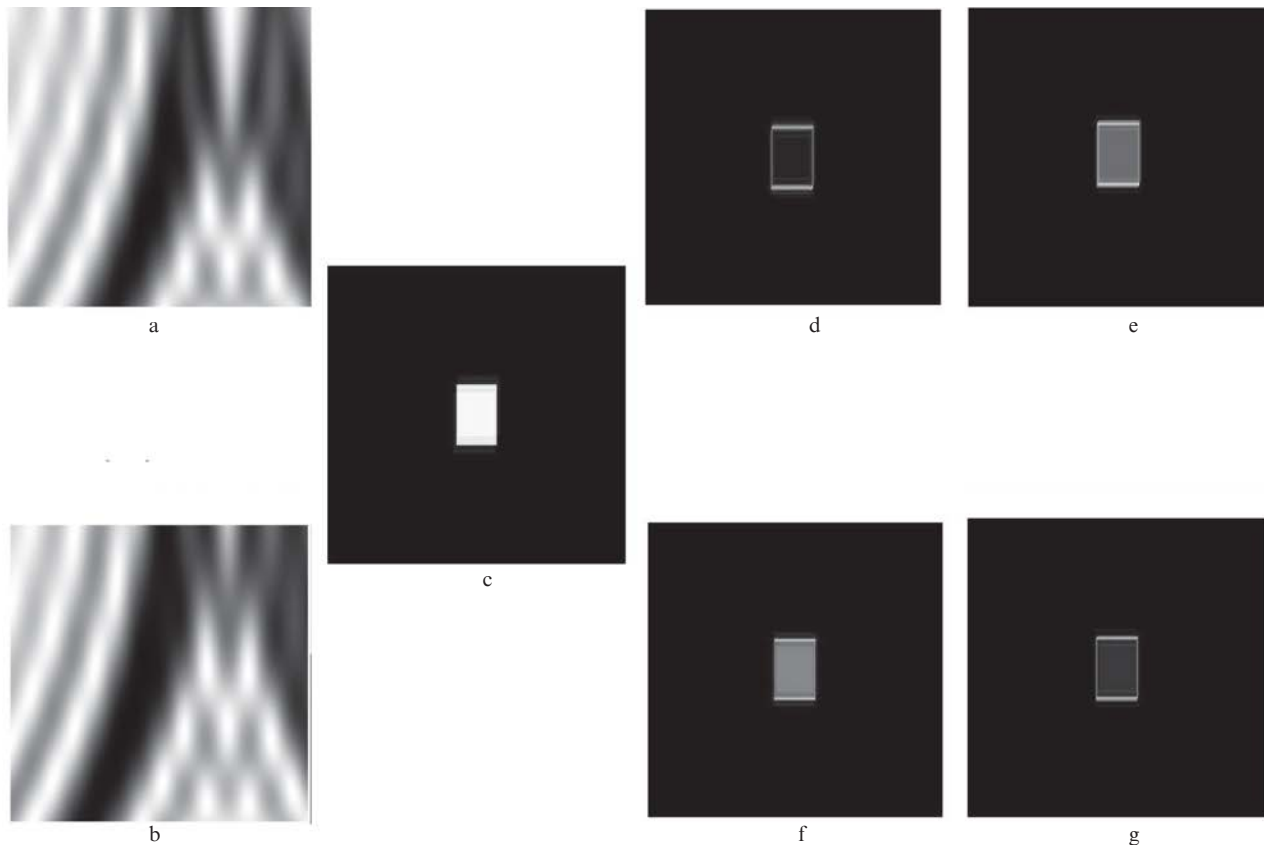
Figure 2. Transfer functions for radiation with wavelengths (a) $\lambda_1 = 0.514 \times 10^{-4}$ cm and (b) $\lambda_2 = 0.488 \times 10^{-4}$ cm, plotted at acoustic powers $P_{ac} = 0.059$ and 0.049 W, respectively; (c) a processed image, and also images transmitted at wavelengths λ_1 and λ_2 after processing using the transfer functions shown in (d, e) Fig. 2a and (f, g) Fig. 2b.

distributions of the amplitudes E_0, E_1, and E_{-1} as functions of the angular distribution of the incident wave amplitude, the sound frequency (these dependences are 'embedded' in the quantities Δk_1 and Δk_2), the light wavelength, the acoustic power, and the crystal parameters.

It follows from the analysis of expressions (1)–(5) that a change in the wavelength λ causes a change in the distributions of the amplitudes of waves diffracted into diffraction orders, since these equations include the wavelength λ, as well as a number of parameters (refractive indices n_o and n_e, pseudotensor gyration G_{33}, acoustic power determined by the parameter p), depending on λ. In this case, the distribution changes in a rather complex way. This leads to the fact that the parameters at which the edges of the image are formed at two wavelengths do not coincide. We add that the transition from one wavelength to another is associated, as a rule, with the need to change several parameters at once. For practical applications, it would be useful to find such regimes of AO diffraction in which this transition occurs by changing only one parameter (for example, the frequency of sound or its power). In this work, we propose a regime in which the transition from one wavelength to another occurs by changing only the acoustic power.

Here are the specific results of processing an image formed using two-colour Ar-laser radiation. The initial parameters for the calculations were taken from [24, 25] in relation to the TeO$_2$ crystal: $n_o = 2.3303$, $n_e = 2.494$, $G_{33} = 3.93 \times 10^{-5}$ for $\lambda_1 = 0.488 \times 10^{-4}$ cm and $n_o = 2.3115$, $n_e = 2.4735$, $G_{33} = 3.69 \times 10^{-5}$ for $\lambda_2 = 0.514 \times 10^{-4}$ cm. In TeO$_2$,

the speed of sound is $V = 617$ m s^{-1}. The following parameters included in expressions (1)–(5) were used in the calculations: $M_2 = 1200 \times 10^{-18}$ s^3 g^{-1}, $L = H = 0.3$ cm; acoustic wave frequency, $f = 57$ MHz (experimental condition); and acoustic power $P_{ac} = 0.059$ W and 0.049 W for λ_1 and λ_2, respectively.

The results of image processing in the form of a rectangle are illustrated in Fig. 2. Figures 2a and 2b show the transfer functions plotted for wavelengths λ_1 and λ_2 at acoustic powers of 0.059 and 0.049 W, respectively. Figure 2c shows the input image, and Figs 2d–2g present the results of its processing: images transmitted at wavelengths λ_1 and λ_2 after processing using the transfer functions shown in Fig. 2a (d, e) and Fig. 2b (f, g). It can be seen that the transfer function in Fig. 2a provides the edge enhancement at λ_1 (Fig. 2d), but does not form the image edge at λ_2 (Fig. 2e). The function in Fig. 2b, on the contrary, provides the edge enhancement at λ_2, but does not form it at λ_1 (Figs 2f and 2g, respectively).

3. Experiment and discussion of its results

An experiment was performed on the basis of the obtained theoretical results. The optical scheme of the experimental setup is shown in Fig. 3. Two-colour optical radiation generated by an Ar laser (L) at wavelengths $\lambda_1 = 0.514 \times 10^{-4}$ cm and $\lambda_2 = 0.488 \times 10^{-4}$ cm is transmitted through an achromatic quarter-wave plate λ/4 and passes through the slit (I). The slit is a square with a side of 0.4 mm and represents an input

image. After the slit, the radiation passes through a system of lenses L1 and L2: the first of them performs the 'direct' Fourier transform, and the second one performs the 'inverse' Fourier transform. The focal length of these lenses is $F = 18$ cm. The distance between the input image I and lens L1 is equal to F, and the distance between lenses L1 and L2 is $2F$. Strictly in the middle between lenses L1 and L2 there is an AO filter (AOF). The output image is formed in the plane P, located at a distance F from lens L2. A lens with a focal length of 5 cm (L3) is used to magnify the image. Then, the radiation passes through the interference filter (IF), which transmits radiation with a wavelength λ_1 and reflects radiation with λ_2. Images at wavelengths λ_1 and λ_2 are observed on screens S1 and S2, respectively. The AO filter is made of a TeO_2 single crystal measuring 1.0, 0.8, and 0.8 cm along the [110], [1$\bar{1}$0], and [001] directions, respectively. A $LiNbO_3$ transducer is glued to the {110} face of the crystal, generating a transverse acoustic wave with a shift along the [1$\bar{1}$0] direction. The transducer had a size of 0.3×0.3 cm, the frequency of sound generation was 57 MHz, and the speed of sound in the crystal was 617 m s^{-1}.

Figure 4. (Colour online) Images transmitted at wavelengths (a, c) $\lambda_1 = 0.514 \times 10^{-4}$ cm and (b, d) $\lambda_2 = 0.488 \times 10^{-4}$ cm, which are observed on screens S1 and S2, respectively; (a, b) in the absence and (c, d) in the presence of a sound wave.
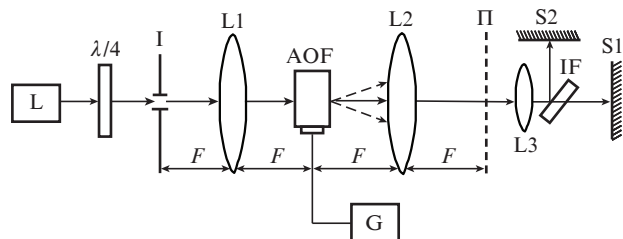

Figure 3. Optical scheme of the experimental setup: (L) source of two-colour radiation; ($\lambda/4$) achromatic quarter-wave plate; (I) original image; (L1, L2) lenses performing the Fourier transform; (AOF) AO filter; (G) generator feeding the AO filter; (P) plane of the formation of the output image; (L3) magnifying lens; (IF) interference filter for a wavelength of 0.514×10^{-4} cm; (S1, S2) screens; F is the focal length of lenses L1 and L2.

At the first stage, by adjusting the AO filter (its orientation and the electric power supplied to the transducer), the conditions were determined under which a two-dimensional contour was formed on the screen for each monochromatic component diffracted into the zero diffraction order. Of several option for adjusting the AO filter, we used the one in which the transition from the wavelength λ_1 to λ_2 with the maintenance of the image contour was carried out by changing only the electric power supplied to the cell. In this case, the orientation of the AO filter did not change. Figure 4 shows photographs of images in green and blue, corresponding to the wavelengths λ_1 and λ_2 of the Ar laser generation, in the absence of a voltage applied to the converter (Figs 4a, 4b) and in its presence (Figs 4c, 4d). The image in Fig. 4c was obtained with an electric power of 0.5 W supplied to the converter, and in Fig. 4d, at a power of 0.35 W. Figures 4c and 4d clearly show two-dimensional edges of the images in green and blue, respectively. Note that when the power is changed by ~0.1 W, the edges are practically blurred. In other words, it was confirmed that there is a regime providing the enhancement of a two-dimensional contour formed at different wavelengths of optical radiation. The edges are formed at different powers of the sound wave.
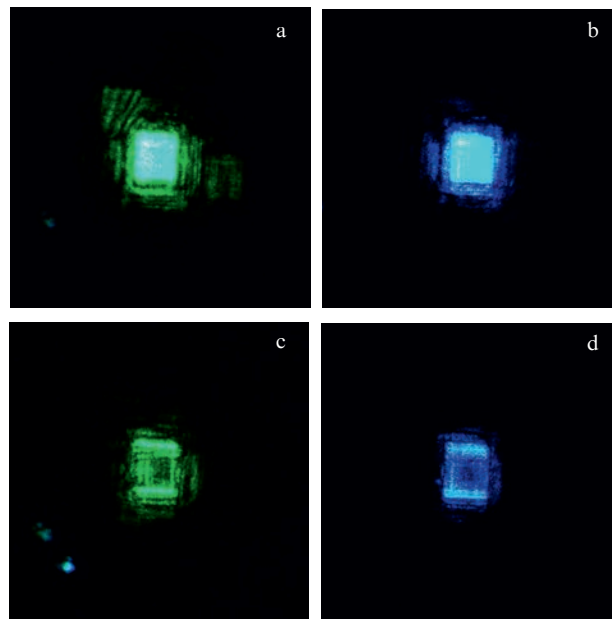
4. Conclusions

Based on the results obtained, we can draw the following conclusions:

1. For two-dimensional processing of images transmitted at two wavelengths of optical radiation, we propose to use an AO spatial frequency filter based on the diffraction of two-colour radiation into two symmetric diffraction orders. The filter operating regime is characterised by a minimum consumption of the acoustic power. The zeroth Bragg order is used as a working diffraction order.

2. It is shown that a two-dimensional contour of an optical image cannot be obtained simultaneously at two wavelengths with the same energy and frequency-angular parameters of the AO filter. A regime of the distribution of the transfer function for two wavelengths (0.488×10^{-4} and 0.514×10^{-4} cm) has been found, in which the transition from one wavelength of light to another while maintaining the operation of two-dimensional image edge enhancement is provided by changing only the acoustic power.

3. The found regime has been experimentally confirmed by the example of the formation of a two-dimensional image edge in the form of a square using two-colour radiation of an Ar laser generating at wavelengths of 0.488×10^{-4} and 0.514×10^{-4} cm. In this case, the AO cell made of TeO_2 serves as a spatial frequency filter, operating at a sound frequency of 57 MHz.

The results obtained can be used for processing optical images using AO filters of spatial frequencies of two-colour optical radiation.

References

1. Case S.K. *Opt. Lett.*, **4** (9), 286 (1979).
2. Athale R.A., van der Gracht J., Prather D.W., Mait J.N. *Appl. Opt.*, **4** (2), 276 (1995).
3. Cao D., Banerjee P.P., Poon T.-Ch. *Appl. Opt.*, **37** (14), 3007 (1998).
4. Balakshy V.I., Voloshinov V.B. *Quantum Electron.*, **35** (1), 85 (2005) [*Kvantovaya Elektron.*, **35** (1), 85 (2005)].
5. Balakshy V.I., Voloshinov V.B., Babkina T.M., Kostyuk D.E. *J. Mod. Opt.*, **52**, 1 (2005).
6. Kostyuk D.E. Cand. Dis. (Moscow, Lomonosov Moscow State University, 2008).
7. Balakshy V.I., Kostyuk D.E. *Appl. Opt.*, **48**, C24 (2009).
8. Yablokova A.A., Machikhin A.S., Batshev V.I., Pozhar V.E., Boritko S.V. *Proc. SPIE*, **11032**, 1103215 (2019).
9. Kotov V.M., Shkerdin G.N., Bulyuk A.N. *Quantum Electron.*, **41** (2), 1113 (2011) [*Kvantovaya Elektron.*, **41** (2), 1113 (2011)].
10. Kotov V.M., Shkerdin G.N., Averin S.V. *Radiotekh.*, **12**, 57 (2012).
11. Kotov V.M., Shkerdin G.N. *Radiotekh. Elektron.*, **58** (10), 1040 (2013).
12. Kotov V.M., Shkerdin G.N., Averin S.V. *Radiotekh. Elektron.*, **61** (11), 1090 (2016).
13. Kotov V.M., Averin S.V., Kuznetsov P.I., Kotov E.V. *Quantum Electron.*, **47** (7), 665 (2017) [*Kvantovaya Elektron.*, **47** (7), 665 (2017)].
14. Kotov V.M., Averin S.V., Kotov E.V., Shkerdin G.N. *Appl. Opt.*, **57** (10), C83 (2018).
15. Magdich L.N., Molchanov V.Ya. *Acousto-Optical Devices and Their Application* (New York: Gordon and Breach, 1989; Moscow: Sov. Radio, 1978).
16. Balakshy V.I., Parygin V.N., Chirkov L.E. *Fizicheskie printsypy akustooptiki* (Physical Principles of Acoustooptics) (Moscow: Radio i Svyaz', 1985).
17. Xu J., Stroud R. *Acousto-Optic Devices: Principles, Design, and Applications* (New York: John Wiley & Sons Inc., 1992).
18. Kotov V.M. *Opt. Spectrosc.*, **77** (3), 437 (1994) [*Opt. Spektrosk.*, **77** (3), 493 (1994)].
19. Kotov V.M. *Tech. Phys.*, **41** (5), 460 (1996) [*Zh. Tekh. Fiz.*, **66** (5), 99 (1996)].
20. Kotov V.M. *Opt. Spectrosc.*, **76** (3), 428 (1994) [*Opt. Spektrosk.*, **76** (3), 479 (1994)].
21. Kotov V.M., Shkerdin G.N., Kotov E.V., Tikhomirov S.A. *Prikl. Fiz.*, **4**, 20 (2011).
22. Kotov V.M., Averin S.V. *Quantum Electron.*, **50** (3), 305 (2020) [*Kvantovaya Elektron.*, **50** (3), 305 (2020)].
23. Kotov V.M. *Akustooptika. Breggovskaya difraktsiya mnogotsvetnogo izlucheniya* (Acousto-optics. Bragg Diffraction of Multicolour Radiation) (Moscow: Yanus-K, 2016).
24. Shaskol'skaya M.P. (Ed.) *Akusticheskie kristally* (Acoustic Crystals) (Moscow: Nauka, 1982).
25. Kizel' V.A., Burkov V.I. *Girotropiya kristallov* (Gyrotropy of Crystals) (Moscow: Nauka, 1980).